Ab Initio Hartree−Fock and Density Functional Studies on the Structures and Vibrations of an Infinite Hydrogen Fluoride Polymer

So Hirata and Suehiro Iwata*

The Graduate University for Advanced Studies and Institute for Molecular Science, Okazaki, Aichi 444-8585, Japan

Received: May 27, 1998

Structural parameters, binding energies, and frequencies of the infrared- and Raman-active vibrations are calculated for an infinite zigzag chain of hydrogen fluoride molecules by ab initio crystal orbital theory with the analytical energy gradient scheme. The Becke−Lee−Yang−Parr (BLYP), Becke3−Lee−Yang−Parr (B3LYP), and Hartree−Fock (RHF) levels are used in conjunction with the 6-311++G(d,p) basis set. Molecular orbital calculations at the BLYP, B3LYP, RHF, and the second-order Møller−Plesset perturbation (MP2) levels with the same basis set are carried out on linear HF oligomers containing up to six molecules, to examine the chain-length dependence of the energetic and structural properties. The predicted chain-length dependence is found to be significantly smaller in the RHF results than in the BLYP and B3LYP results. The RHF level substantially underestimates the downward frequency shifts in the intramolecular H−F stretching modes on going from the monomer to the polymer, while the shifts calculated at the BLYP and B3LYP levels are much closer to the experimental findings, although they are slightly overestimated. The RHF level strongly underestimates the intramolecular H−F bond length and overestimates the intermolecular F···H and F···F distances of the HF polymer, while the structural parameters predicted at the BLYP and B3LYP levels are in good agreement with the experimental results. It is concluded that the RHF level seriously underestimates the cooperative binding effects of consecutive hydrogen bonds, whereas the BLYP and B3LYP levels slightly overestimate this behavior; but these latter levels provide much better description than the former. Vibrational assignment of librational modes of HF crystals is reexamined on the basis of the calculated frequencies. The observed frequencies of the librational and pseudo-translational modes fall between the corresponding frequencies calculated at the RHF and density functional levels.

Introduction

It is well recognized that the energetic and structural properties of consecutively hydrogen-bonded systems (···X−H···X−H···X−H···) exhibit "cooperative" or "nonadditive" behavior.[1−8] For instance, the binding energy per hydrogen bond increases as the number of constituent X−H molecules increases. The intermolecular H···X distances shorten and the intramolecular X−H bonds lengthen as the chain becomes longer, which accompanies a decrease in the frequencies of the X−H stretching modes. The dipole moments of hydrogen-bonded chains are usually larger than a simple vector addition of the dipole moment of a monomer would suggest. Quantitative knowledge of the cooperativity is essential in studying the structures and dynamics of hydrogen-bonded systems in the condensed phase.

The cooperative behavior is most clearly illustrated by the linear or cyclic hydrogen-bonded chains of hydrogen fluoride (HF) molecules.[3,5,9−17] The intermolecular binding in HF clusters is categorized into moderately strong hydrogen bonds,[5] and the crystalline HF is constructed from one-dimensional zigzag chains $(HF)_\infty$ of HF molecules.[18−20] The intermolecular F···F distance of $(HF)_\infty$ is 2.49−2.50 Å (refs 18 and 19), which is substantially shorter than the F···F distance (2.72−2.79 Å) (refs 21 and 22) of the neutral dimer $(HF)_2$. The frequencies of the H−F stretching modes decrease by several hundreds of cm^{-1} on going from $(HF)_2$ (ref 23) to $(HF)_\infty$ (refs 20, 24−30).

The most intensive investigations on the cooperativity of the hydrogen bonds in HF clusters were carried out by Karpfen and Yanovitskii.[14,15] They examined the chain-length dependence of the H−F and F···F distances, frequencies of the H−F stretching modes, and other properties for neutral, protonated, and deprotonated HF clusters. In these studies, the authors employed the Hartree−Fock approximation with the 4-31G, 6-31G(d,p), and 6-311++G(2d,p) basis sets. The calculated chain-length dependence was found to be systematic, and it turned out that the calculated bond lengths and frequencies converged very slowly to the corresponding values of $(HF)_\infty$. Therefore, it is hardly possible to obtain the structures or vibrational frequencies of $(HF)_\infty$ by extrapolation from those of oligomers with reasonably large basis sets or theoretical levels which incorporate the effects of electron correlation.

An alternative, and in principle more accurate and efficient, method to calculate the structures and vibrational frequencies of infinite chains is provided by ab initio crystal orbital theory.[31−34] Several papers have been published so far which have dealt with $(HF)_\infty$ on the basis of ab initio crystal orbital theory[35−41] or periodic density functional theory using local exchange-correlation functionals.[42,43] Among them, the paper written by Beyer and Karpfen[37] has been the only one which reported the optimized structural parameters and vibrational frequencies of $(HF)_\infty$ obtained with reasonably large basis sets. These authors employed the Hartree−Fock approximation in conjunction with the Gaussian lobe basis sets. The H−F bond length of $(HF)_\infty$ calculated with the largest basis set they used was, however, significantly shorter than the experimental results. Correspondingly, the calculated F···F bond length was much

10.1021/jp982383h CCC: $15.00
Published on Web 10/03/1998

longer than the experimental values, and the calculated frequencies of the H−F stretching modes were overestimated by more than 700 cm^{-1}.

It is probable that these discrepancies are ascribed to the neglect of electron correlation. Recently, Karpfen[17] has extended the investigations of HF clusters to second-order Møller−Plesset perturbation (MP2) theory and several variants of density functional theory with the 6-311++G(2d,p) basis set. However, there seems to be no calculation on the structure and vibrational frequencies of $(HF)_\infty$ using correlated theoretical levels with reasonably large basis sets. Such calculations are of great importance, since they directly provide us with quantitative information about the cooperativity of consecutive hydrogen bonds in the solid state. This is especially true for $(HF)_\infty$ because the structures and vibrations of the dimer have thoroughly been investigated both experimentally and theoretically (see, e.g., refs 10, 17, 44, 45, and references therein). The performance of a theoretical method as a means to study the hydrogen-bonded systems will be best judged on the basis of the crystal orbital calculations, since the cooperative effects are more pronounced in the condensed phase than in small clusters.

In this article, we present the results of ab initio Hartree−Fock and density functional crystal orbital calculations on $(HF)_\infty$. The structural parameters are optimized, and frequencies of the infrared- and Raman-active vibrations are calculated using the gradient-corrected Becke−Lee−Yang−Parr (BLYP)[46−48] and the hybrid Becke3−Lee−Yang−Parr (B3LYP)[49] functionals as well as the spin-restricted Hartree−Fock (RHF)[50] approximation in conjunction with the 6-311++G(d,p) basis set. Our choice of the exchange-correlation functionals and basis set has been made on the basis of previous density functional studies of the HF dimer.[51−53] To examine the chain-length dependence of the energetic and structural properties, ab initio molecular orbital calculations at the RHF, BLYP, B3LYP, and MP2 levels using the same basis set are carried out for HF oligomers up to the hexamer in the linear chain configuration. The effects of electron correlation, as taken into account at the BLYP and B3LYP levels, on structural parameters, binding energies, and vibrational frequencies are elucidated. The assignment of the observed infrared and Raman bands of HF crystals is also discussed on the basis of the calculated results.

Method of Calculations

Oligomer Calculations. Ab initio molecular orbital calculations on the linear HF oligomers up to the hexamer were carried out with the Gaussian 94 program.[54] The geometry optimizations and vibrational frequency calculations were performed at the RHF, BLYP, B3LYP, and MP2 levels with the internally stored 6-311++G(d,p) basis set. We specified the "6d" option, which requests that six Cartesian d-type functions instead of five pure d-type functions be used, to make the basis sets used in molecular orbital and crystal orbital calculations identical. All the electrons were correlated in the MP2 calculations.

In the geometry optimizations of the linear oligomers, we assumed the planarity of the molecules and optimized all the remaining structural parameters. Anharmonic vibrational frequencies of the monomer were calculated by the three-term finite-difference method[55] using one-dimensional potential energy curves computed by changing the H−F distance at 0.04 Å intervals in the range of 0.5−1.5 Å.

The intermolecular binding energy of the dimer (trimer) was obtained at each theoretical level as the total energy of the dimer (trimer) minus twice (three times) the total energy of the isolated monomer at their respective optimized structures. We estimated the basis set superposition errors (BSSE) in the binding energies of the dimer and trimer by the function counterpoise method of Boys and Bernardi,[56] taking into account the structural relaxation of the monomer upon the dimer or trimer formation.[57] The BSSE correction to the binding energy of the trimer was estimated by using eq 6 in the paper of Turi and Dannenberg.[58]

Polymer Calculations. The geometry optimizations and vibrational frequency calculations of infinite zigzag HF chains were carried out using the analytical energy gradients of ab initio crystal orbital theory. Density functional theory using the BLYP and B3LYP functionals as well as RHF theory was employed with the 6-311++G(d,p) basis set. The formulas for the self-consistent-field (SCF) procedures of ab initio crystal orbital theories are given in refs 31−34. Analytical energy gradient formulas for crystal orbital theory were first derived and implemented by Teramae et al.[59,60] at the Hartree−Fock level, and recently we extended them to the density functional and hybrid Hartree−Fock/density functional levels.[61] In our previous density functional crystal orbital studies,[61−63] we expanded the electron density by auxiliary basis sets and evaluated the Coulomb repulsion energies with two- and three-index electron repulsion integrals (ERIs) instead of four-index ERIs.[64,65] In the present study, however, we evaluated the Coulomb repulsion energies with four-index ERIs in order that we can compare the results of the crystal orbital calculations directly with those of the molecular orbital calculations. The contributions of long-range electrostatic interactions to total energies and to Fock matrix elements were evaluated by the multipole expansion technique developed by Delhalle et al.[66] Accordingly, we employed different formulas for the total energies and analytical energy gradients of density functional crystal orbital theory from those given in our recent paper.[61] For the sake of completeness, the formulas used in the present study are given in the Appendix.

A translational repeat unit of $(HF)_\infty$ contains two HF molecules. The geometry optimizations of the polymer were performed with the analytical energy gradients by taking an HF unit as the reference unit cell and by making use of the screw axis symmetry. Four-index ERIs were evaluated by using the 8th, 10th, and 16th neighbor approximations for the BLYP, B3LYP, and RHF calculations, respectively. The use of different cutoff radii for different theoretical levels is justified because the exchange-correlation matrix elements decay more rapidly than the exact-exchange matrix elements. The criterion for the convergence of density matrix elements was set to 10^{-8}. The threshold value for the residual energy gradients was 10^{-5} hartree/bohr.

In the vibrational frequency calculations, we adopted a translational repeat unit, i.e., an $(HF)_2$ unit, as the reference unit cell in order to obtain frequencies of all the infrared- and Raman-active modes. Accordingly, we employed the 4th, 6th, and 10th neighbor approximations for the BLYP, B3LYP, and RHF calculations, respectively. Force constants were evaluated by numerical differentiation of the analytical energy gradients. Step size used in the numerical differentiation was 0.04 bohr. We employed the Namur cutoff criterion with multipole expansion corrections,[66,67] taking into account the dipole−dipole and charge−quadrupole interaction corrections to total energies and to Fock matrix elements. The other parameters of calculations such as the number of wave vector sampling points and the numerical quadratures and grids used in numerical integration were the same as those used in our previous studies.[61−63]

The binding energy of $(HF)_\infty$ was obtained at each theoretical level as the difference between the total energy of the polymer per HF unit and the total energy of the isolated monomer at

TABLE 1: Equilibrium Bond Length (in Units of Å) and Harmonic and Anharmonic Vibrational Frequencies (in Units of cm^{-1}) of an HF Molecule

	BLYP	B3LYP	RHF	MP2	expt
H−F bond length	0.933	0.922	0.898	0.917	0.917[a]
harmonic frequencies	3939	4098	4491	4200	4138[a]
anharmonic frequencies	3758	3919	4319	4021	3961[b]

[a] Reference 68. [b] Reference 73.

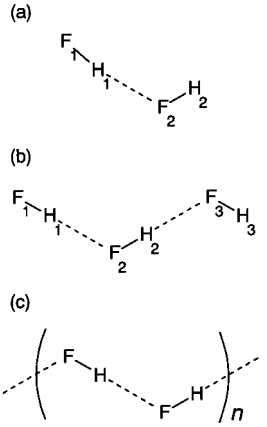

Figure 1. Linear hydrogen-bonded (a) dimer, (b) trimer, and (c) polymer of hydrogen fluoride molecules.

their respective optimized geometries. The BSSE were evaluated by function counterpoise method.[56−58] We computed the total energy of the monomer with the bond length being equal to that of $(HF)_\infty$ using the basis set of the whole polymer chain. Ghost basis functions were placed within the third nearest HF unit cells at both sides of the reference unit cell.

Results and Discussion

Structures. In Table 1, the equilibrium bond lengths of an HF molecule calculated at the BLYP, B3LYP, RHF, and MP2 levels are compared with experimental results.[68] The H−F bond length calculated at the RHF level (0.898 Å) is significantly shorter than the experimental value (0.917 Å), whereas the bond length predicted at the BLYP level (0.933 Å) is too long. At the B3LYP and MP2 levels, the calculated H−F bond lengths agree reasonably well with the experimental value. The errors that are visible in the monomer description at a given theoretical level are carried over to longer oligomers and polymer (vide post).

It has been established by microwave molecular beam experiments[21,22] that the lowest energy configuration of $(HF)_2$ is bent C_s structure with nearly linear F−H···F hydrogen bond, as illustrated in Figure 1. All the theoretical models employed in this study (BLYP, B3LYP, RHF, and MP2) correctly reproduce the bent configuration as the global minimum, provided that the 6-311++G(d,p) basis set is used (see also ref 51−53). The optimized structural parameters of the HF dimer are compiled in Table 2 along with the experimental data taken from refs 21, 22, and 69. It is seen from Table 2 that the calculated intramolecular H−F bond lengths increase in the same order (RHF < MP2 < B3LYP < BLYP) as the calculated bond lengths of the monomer. The calculated intermolecular H···F and F···F distances are dependent on the theoretical level employed to a larger extent. The F···F distance predicted at the RHF level (2.826 Å) is longer than that obtained at the B3LYP level (2.748 Å) by as much as 0.078 Å, while the F···F distances calculated at the BLYP and MP2 levels fall between these two values. It is difficult to judge which theoretical level yields the best F···F distance on the basis of the comparison between the calculations and experiments due to the large uncertainties in the experimental data. The $F_2F_1H_1$ angles calculated with all of four levels of approximation are within the range of experimental errors. On the other hand, the calculated $F_1F_2H_2$ angles vary substantially with the theoretical levels, and the RHF result seems to be too large as compared with the experimental values.

The most stable structure of $(HF)_3$ in the vapor phase is a cyclic configuration with the C_{3h} symmetry, as has been determined by experimental and theoretical studies (see, e.g., ref 17 and references therein). The trimer in the linear open chain configuration (see Figure 1), therefore, corresponds to either a local minimum or a saddle point on the potential energy surface. The BLYP and B3LYP levels predict that the linear $(HF)_3$ oligomer is a local minimum, whereas the RHF and MP2 levels indicate that this configuration is a first-order saddle point. The calculated bond distances of $(HF)_3$ are given in Table 3. The calculated intramolecular H−F bond lengths depend on the theoretical levels in the way parallel to that found in the monomer and dimer results.

At each theoretical level, the calculated hydrogen-bond distances of the trimer are substantially shorter than that of the dimer. For instance, at the B3LYP level, the calculated $H_1\cdots F_2$ and $H_2\cdots F_3$ distances of the trimer are 1.771 and 1.743 Å, respectively, which are shorter by 0.061 and 0.089 Å than the calculated H···F distance of the dimer (1.832 Å). These reductions in the hydrogen-bond distances can be regarded as a manifestation of the cooperativity. We observe the similar amounts of reductions at the MP2 (0.062 and 0.087 Å) and at the BLYP level (0.062 and 0.091 Å). However, the values obtained at the RHF level (0.054 and 0.074 Å) are smaller than those obtained at the correlated levels.

One of the normal modes of $(HF)_3$ calculated at the RHF and MP2 levels has an imaginary frequency. That mode corresponds to localized out-of-plane motion of the terminal (non-hydrogen-bonded) hydrogen atom.[14] For longer oligomers, some of the normal modes obtained at the density functional levels as well as at the RHF and MP2 levels also have imaginary frequencies. These imaginary frequencies are always associated with localized motion of terminal molecules, and hence we can safely expect that the structural parameters and vibrational frequencies of the central part of HF oligomers approach the

TABLE 2: Structural Parameters of an Open HF Dimer[e]

structural parameter[a]	BLYP	B3LYP	RHF	MP2	expt
F_1-H_1 bond length	0.941	0.929	0.901	0.921	
$H_1\cdots F_2$ bond length	1.847	1.832	1.933	1.876	
F_2-H_2 bond length	0.936	0.925	0.900	0.920	
$F_1\cdots F_2$ bond length	2.772	2.748	2.826	2.788	2.79 ± 0.05,[b] 2.72 ± 0.03[c]
$F_2F_1H_1$ angle	8.5	7.9	6.5	6.5	10 ± 6,[c] 7 ± 3[d]
$F_1F_2H_2$ angle	113.6	116.6	126.8	121.0	117 ± 6,[c] 120 ± 2[d]

[a] Atoms are numbered as $F_1-H_1\cdots F_2-H_2$. [b] Reference 21. [c] Reference 22. [d] Reference 69. [e] Bond lengths in Å and bond angles in deg.

TABLE 3: Structural Parameters of an Open HF Trimer[b]

structural parameter[a]	BLYP	B3LYP	RHF	MP2
F_1-H_1 bond length	0.944	0.932	0.903	0.923
$H_1\cdots F_2$ bond length	1.785	1.771	1.879	1.814
F_2-H_2 bond length	0.948	0.935	0.905	0.926
$H_2\cdots F_3$ bond length	1.756	1.743	1.859	1.789
F_3-H_3 bond length	0.937	0.926	0.901	0.921

[a] Atoms are numbered as $F_1-H_1\cdots F_2-H_2\cdots F_3-H_3$. [b] Bond lengths in Å and bond angles in deg.

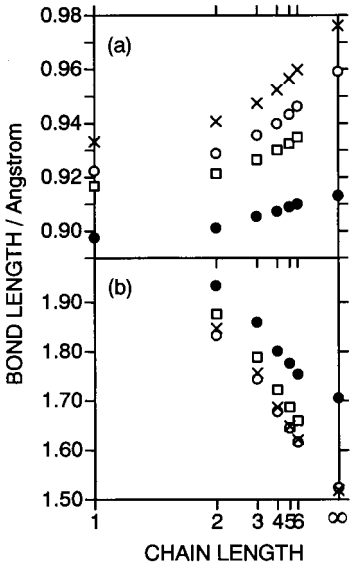

Figure 2. Calculated (a) intramolecular H−F bond lengths and (b) H···F hydrogen-bond distances of hydrogen fluoride oligomers and polymer plotted as a function of the inverse of chain length. Crosses: BLYP; open circles: B3LYP; filled circles: RHF; squares: MP2. Only the longest H−F and the shortest H···F distances are used.

corresponding values of an infinite polymer with increasing chain length.

In Figure 2, the intramolecular H−F bond lengths and the H···F hydrogen-bond distances are plotted versus the inverse of chain length. Only the longest H−F bond length and the shortest H···F distance of each oligomer are used. The corresponding bond lengths of the HF polymer directly obtained from the crystal orbital calculations at the BLYP, B3LYP, and RHF levels are also included. It can be seen that the H−F bond lengths calculated at the BLYP and B3LYP levels change with increasing chain length to a greater extent than those calculated at the RHF level. The BLYP and B3LYP calculations indicate that there is a substantial elongation in the longest H−F bond on going from the hexamer to the polymer, while the RHF calculations show that the bond lengths mostly converge at the hexamer. The chain-length dependence predicted at the MP2 level seems to be intermediate between the density functional results and the RHF result. The chain-length dependence of the H···F hydrogen-bond distances is by an order of magnitude larger than that of the intramolecular H−F bond lengths. The H···F distances calculated with the BLYP and B3LYP levels coincide with each other. The RHF level again predicts smaller chain-length dependence than the BLYP and B3LYP levels do. The results obtained from the MP2 calculations seem to be closer to the density functional results than to the RHF results.

The optimized structural parameters of the HF polymer obtained at the RHF, BLYP, and B3LYP levels are compiled in Table 4 with the experimental data of crystalline HF taken from refs 18, 19, and 70. In this table, we include the results of previous crystal orbital calculations of Beyer and Karpfen[37] at the RHF level. They employed three different basis sets, i.e., basis sets I, II, and III. Size of the basis sets is in the order: III ≈ 6-311++G(d,p) > II > I.

First, we point out that the structural parameters obtained by Beyer and Karpfen with basis set III are in reasonable agreement with our result using the basis set of comparable size, i.e., 6-311++G(d,p). The effects of electron correlation, as taken into account at the BLYP and B3LYP levels, are profound on the structural parameters. The H−F bond lengths calculated at the BLYP and B3LYP levels are 0.976 and 0.959 Å, respectively, which are significantly longer than the RHF value (0.913 Å). The measured H−F bond lengths are 0.97 ± 0.02 Å from the neutron diffraction study[19] and 0.95 ± 0.03 Å from the NMR study.[70] The RHF level underestimates the H−F bond length of $(HF)_\infty$, as it does for the isolated monomer, while the bond lengths obtained from the BLYP and B3LYP calculations are within the experimental errors. Similarly, the RHF level substantially overestimates the F···H and F···F distances, whereas the BLYP and B3LYP levels yield calculated distances which are very close to the experimental data. The H−F, F···H, and F···F lengths calculated at the RHF level with basis set I are apparently in good agreement with the experiments, but this coincidence is fortuitous and is due to the cancellation of the errors arising from the small basis set used and from the neglect of electron correlation. The FFF angle obtained at the RHF level (132.0 degree) is much larger than the values determined by X-ray diffraction (120.1 degrees) or by neutron diffraction (116 degrees) technique. The BLYP and B3LYP calculations reproduce the experimental angles reasonably well. At the RHF level, the translational period is also greatly overestimated as compared with the experimental results, owing to the too large values of the F···F distance and FFF angle predicted at this level. The BLYP and B3LYP levels, in contrast, reproduce the experimental results quantitatively.

If we take the H−F bond length determined by neutron diffraction technique[19] as a reference value, the discrepancy between the calculated bond length and the reference value amounts to about 0.06 Å at the RHF level. Since the RHF level underestimates the H−F bond length of the isolated monomer by about 0.02 Å, the remaining discrepancy of 0.04 Å is ascribed to the underestimation of the chain-length dependence of the H−F bond length. This result indicates that the inclusion of electron correlation is essential in describing the cooperativity of consecutive hydrogen bonds quantitatively. Likewise the discrepancy between the F···F distance of the HF polymer calculated at the RHF level and the observed value is at least partly ascribable to the underestimation of the cooperative behavior.

Binding Energies. The calculated binding energies of $(HF)_2$ and $(HF)_3$ are listed in Tables 5and 6, respectively. The RHF level predicts the weakest hydrogen bond for $(HF)_2$ and the B3LYP level the strongest hydrogen bond among the theoretical levels employed here. As a consequence, the H···F hydrogen-bond distance calculated at the B3LYP levels is the shortest and that at the RHF level is the longest (vide ante). Since these binding energies inevitably contain the BSSE, which amount to a few kJ mol^{-1}, all the calculated values for $(HF)_2$ may be too small as compared with the experimental results.[71,72] In particular, the BSSE in the MP2 result is roughly twice as large as those in the RHF and density functional results. Although the binding energies directly obtained from the MP2 calculations, which contain BSSE, are apparently in good agreement with the experimental values, they become systematically

TABLE 4: Structural Parameters of an Infinite HF Polymer[h]

	crystal orbital calculation						
	BLYP[a]	B3LYP[a]	RHF[a]	RHF[b]	RHF[c]	RHF[d]	expt
H−F bond length	0.976	0.959	0.913	0.918	0.917	0.942	0.97 ± 0.02,[e] 0.95 ± 0.03[f]
F···H bond length	1.519	1.524	1.705	1.69	1.660	1.526	1.53 ± 0.02[e]
F···F bond length	2.495	2.483	2.618	2.60	2.577	2.468	2.50 ± 0.01,[e] 2.49 ± 0.01[g]
FHF angle	178.5	178.6	177.9	178.0	178.1	177.7	176[e]
FFF angle	120.2	122.8	132.0	129.7	130.2	141.9	116,[e] 120.1[g]
translational period	4.326	4.361	4.783	4.707	4.675	4.666	4.26 ± 0.01,[e] 4.32 ± 0.01[g]

[a] Obtained in this study using the 6-311++G(d,p) basis set. [b] Obtained by Beyer and Karpfen (ref 37) with basis set III (see text). [c] Obtained by Beyer and Karpfen (ref 37) with basis set II (see text). [d] Obtained by Beyer and Karpfen (ref 37) with basis set I (see text). [e] Reference 19. [f] Reference 70. [g] Reference 18. [h] Bond lengths in Å and bond angles in degree.

TABLE 5: Binding Energy (in Units of kJ mol^{-1}) of an Open HF Dimer

	BLYP	B3LYP	RHF	MP2	expt
binding energy	19.9	21.2	18.2	19.6	19.1 ± 1.2 [a]
binding energy + ΔZPE[c]	12.6	13.9	11.3	12.6	12.74 ± 0.06 [b]
BSSE[d]	2.3	2.2	1.7	3.8	

[a] Reference 71. [b] Reference 72. [c] Correction due to the zero-point vibrational energy. [d] Basis set superposition error estimated by the function counterpoise method.

TABLE 6: Binding Energy (in Units of kJ mol^{-1}) of an Open HF Trimer

	BLYP	B3LYP	RHF	MP2
binding energy	46.2	48.9	41.5	45.1
binding energy + Δ ZPE[a]	31.5	34.0	27.7	31.0
BSSE[b]	4.9	4.8	3.8	8.9

[a] Correction due to the zero-point vibrational energy. [b] Basis set superposition error estimated by the function counterpoise method.

TABLE 7: Binding Energy (in Units of kJ mol^{-1}) of an Infinite HF Polymer

	BLYP[a]	B3LYP[a]	RHF[a]	RHF[b]	RHF[c]	RHF[d]
binding energy	35.5	36.4	28.5	27.2	31.8	51.9
BSSE[e]	3.3	3.2	2.5			

[a] Obtained in this study using the 6-311++G(d,p) basis set. [b] Obtained by Beyer and Karpfen (ref 37) with basis set III (see text). [c] Obtained by Beyer and Karpfen (ref 37) with basis set II (see text). [d] Obtained by Beyer and Karpfen (ref 37) with basis set I (see text). [e] Basis set superposition error estimated by the function counterpoise method.

smaller than the experimental values if we subtract BSSE from them. It should be kept in mind that the calculated structural parameters and vibrational frequencies also contain errors resulting from the BSSE in the binding energies.

Binding energies per hydrogen bond increase with increasing chain length, which is another manifestation of the cooperativity of hydrogen bonds. At each theoretical level, the calculated binding energy of $(HF)_3$ is substantially larger than twice the calculated binding energy of $(HF)_2$. The ratio of the binding energy of $(HF)_3$ to that of $(HF)_2$ is the smallest in the RHF result (228%), whereas the ratios obtained with the BLYP, B3LYP, and MP2 levels are within the range of 230−232%. We consider that this result also reflects underestimation of the cooperativity at the RHF level.

The calculated binding energies of the HF polymer are listed in Table 7. Again, we observe a reasonable agreement between the RHF/6-311++G(d,p) result (28.5 kJ mol^{-1}) obtained in this study and the RHF/basis set III result (27.2 kJ mol^{-1}) of Beyer and Karpfen. The BLYP and B3LYP levels predict substantially larger binding energies than the RHF level does. The differences between the density functional results and the RHF result, which amount to 7−8 kJ mol^{-1}, are at least partly traced back to the underestimation of the chain-length dependence of the binding energies at the RHF level.

TABLE 8: Vibrational Frequencies (in Units of cm^{-1}) of an Open HF Dimer[d]

mode	BLYP	B3LYP	RHF	MP2	expt
ν_1 (A′)	3901 (38)	4061 (37)	4455 (36)	4163 (37)	3929 (32)[a]
ν_2 (A′)	3785 (154)	3962 (136)	4411 (80)	4106 (94)	3868 (93)[a]
ν_3 (A′)	579	572	503	538	
ν_4 (A″)	455	456	435	421	370,[b] 400[c]
ν_5 (A′)	222	210	192	203	189[c]
ν_6 (A′)	157	154	141	146	128[c]

[a] Reference 23. [b] Reference 74. [c] References 75−77. [d] The values in parentheses are the frequency shifts from the monomer.

Vibrational Frequencies. The calculated harmonic and anharmonic frequencies of the H−F stretching mode of an HF molecule are compared with the observed frequencies[68,73] in Table 1. The frequencies calculated at the RHF level are overestimated by about 350 cm^{-1}, which is consistent with the too short H−F bond length predicted at this level of theory. At the MP2 level, the calculated frequencies become closer to the observed ones although they are still overestimated by 60 cm^{-1}. The frequencies computed at the BLYP level are too low as compared with the observed frequencies. The results obtained at the B3LYP level are between those obtained at the RHF and BLYP levels and are in reasonably good agreement with the experimental results as well as with the MP2 results. The differences between the harmonic and anharmonic frequencies predicted at the BLYP, B3LYP, RHF, and MP2 levels are 181, 179, 172, and 179 cm^{-1}, respectively, and are in good agreement with the observed frequency difference of 177 cm^{-1}.

In Table 8, the calculated harmonic frequencies of $(HF)_2$ are compared with the measured frequencies.[23,74−77] The frequencies of the H−F stretching modes shift downward on going from the monomer to the dimer. All the theoretical levels reproduce reasonably well the observed frequency shift for ν_1 mode (32 cm^{-1}), which primarily consists of the stretching motion of the proton acceptor molecule. The ν_2 mode is approximately regarded as the stretching motion of the proton donor molecule, and the large frequency shift (93 cm^{-1}) observed for this mode reflects the strong hydrogen-bond interactions between the two HF molecules. The RHF level predicts too small a frequency shift (80 cm^{-1}) as compared with the experimental value, indicating that this level of theory underestimates the hydrogen-bond interactions. The frequency shifts predicted at the BLYP and B3LYP levels are, on the other hand, substantially overestimated. The MP2 level provides the calculated frequency shift of 94 cm^{-1} which is in good agreement with the experimental value. These results suggest that the BLYP and B3LYP levels tend to overestimate the hydrogen-bond interactions, while the MP2 level describe these interactions reasonably well. The calculated frequencies of the intermolecular vibrations

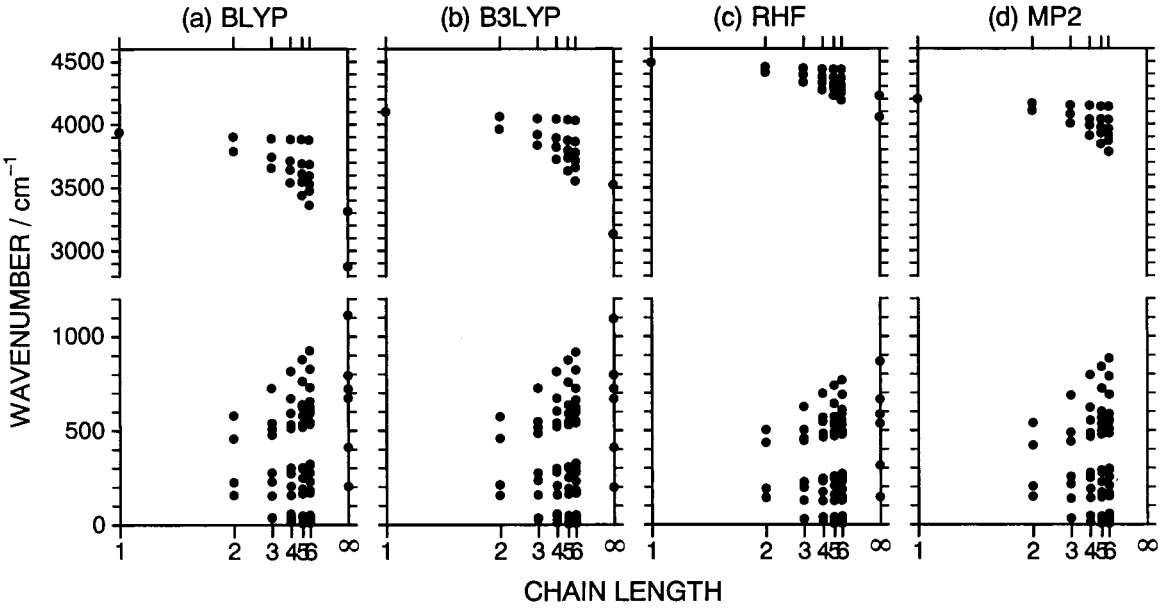

Figure 3. Vibrational frequencies of hydrogen fluoride oligomers and polymer calculated at the (a) BLYP, (b) B3LYP, (c) RHF, and (d) MP2 levels plotted as a function of the inverse of chain length.

increase in the same order (RHF < MP2 < B3LYP < BLYP) as the frequency shifts increase, except for the out-of-plane (ν_4) mode. At all the theoretical levels, the calculated frequencies of the intermolecular vibrations are higher than the observed.[74−77] It should be noted, however, that the "BSSE-free" frequencies would be lower than these calculated frequencies.

The convergence behavior of the vibrational frequencies of the HF oligomers is depicted in Figure 3. In the 2800−4600 cm^{-1} region, the lowest-frequency mode of each oligomer corresponds to the in-phase H−F stretching vibration, whose infrared intensity is the largest in each oligomer. These in-phase H−F stretching vibrations approach the symmetric H−F stretching mode of the polymer as the chain length increases. The highest-frequency mode of each oligomer, on the other hand, is the localized motion of a terminal HF molecule, and its frequency is relatively insensitive to the chain length. The corresponding mode does not exist in the polymer. The absolute values of the H−F stretching frequencies depend strongly on the theoretical levels and are in the order BLYP < B3LYP < MP2 < RHF. This order is determined by the errors that already appear in the monomer results. The chain-length dependence is substantially smaller in the RHF results than in the results obtained at the correlated levels. The chain-length dependence predicted at the BLYP and B3LYP levels is almost the same with each other in magnitude, while that at the MP2 level is again intermediate between the density functional results and the RHF result. The vibrational frequencies in the region below 1200 cm^{-1} are primarily determined by the hydrogen-bond interactions. The RHF level yields invariably lower frequencies for these modes than the other three levels. Among the BLYP, B3LYP, and MP2 results, in contrast, not only the absolute values but also the chain-length dependence of the calculated frequencies in this region agree well with one another.

The calculated frequencies of the infrared- and Raman-active vibrations of $(HF)_\infty$ and $(DF)_\infty$ are compared with the observed frequencies of HF and DF crystals in Table 9. Normal coordinates of these modes are depicted in Figure 4. Infrared spectra of HF crystals were first reported by Giguère and Zengin[24] and subsequently by Sastri and Hornig[20] and by Kittelberger and Hornig.[25] Raman spectra were measured by Anderson et al.,[26,27] and the external-pressure dependence of the spectra has also been studied by Lee et al.,[28] by Jansen et al.,[29] and by Pinnick et al.[30] Boutin et al.[78] and Axmann et al.[79] recorded the inelastic neutron scattering from HF crystals in the region below 600 cm^{-1}. The experimental data in Table 9 are taken from refs 25, 26, and 30. The normal modes are classified into stretching (S), librational (L), and pseudo-translational (T) vibrations according to their vibrational patterns. Among them, the assignment of the observed bands has been established for the stretching and pseudo-translational vibrations.[25] For the librational modes, no consensus on the assignment has been reached among the authors.[25−27,30,79,80]

In Table 9, we include the results obtained by Beyer and Karpfen at the RHF level with basis sets I and II. We can find systematic basis-set dependence of the calculated frequencies in the results of Beyer and Karpfen and our results; as the basis set becomes larger, frequencies of the stretching modes become higher, and frequencies of the librational and pseudo-translational modes become lower. There are substantial changes in the vibrational frequencies on going from basis set II of Beyer and Karpfen to the 6-311++G(d,p) basis set.

In the H−F stretching region (3000−3600 cm^{-1}) of the HF crystals, four infrared absorption bands have been observed.[20,24,25] Among them, two weaker bands were assigned as combination bands of the other two intense fundamental absorption bands and a lattice band near 200 cm^{-1} (ref 25). The two fundamental absorption bands in this frequency region are the symmetric S(A_1) and antisymmetric S(B_1) intramolecular H−F (D−F) stretching vibrations, the former being more intense than the latter.

It is seen from the table that the frequencies of S(A_1) and S(B_1) modes calculated at the RHF level are too high as compared with the experiments. The deviations between the calculations and experiments are as large as about 1000 cm^{-1} for the S(A_1) mode of $(HF)_\infty$. The splitting of these two modes is also greatly underestimated at this level. The observed splittings are 340 cm^{-1} for $(HF)_\infty$ and 230 cm^{-1} for $(DF)_\infty$, whereas the RHF level yields 172 and 123 cm^{-1}. The predicted too small splittings indicate that the RHF level underestimates the hydrogen-bond interactions. As expected from Figure 3, the RHF level also underestimates the downward shift in the stretching frequencies from the isolated monomer to the

TABLE 9: Frequencies (in Units of cm^{-1}) of the Infrared- and Raman-Active Vibrations of an Infinite HF Polymer

	crystal orbital calculation					expt		
mode	BLYP[a]	B3LYP[a]	RHF[a]	RHF[b]	RHF[c]	infrared[d]	Raman[e]	Raman[f]
				$(HF)_\infty$				
$S(B_1)$	3310	3521	4226	4170	3675	3406	3386	3376 ± 5
$S(A_1)$	2874	3128	4054	3967	3357	3067	3045	3027 ± 6
$L(B_1)$	1112	1093	866	1007	1025	975−1025	943	
$L(B_2)$	792	795	665	716	867	792	742	776 ± 1
$L(A_2)$	721	722	585	563	729	inactive	687	722 ± 1
$L(A_1)$	671	668	537	604	702	553	569	566 ± 1
$T(B_1)$	410	409	312	386	490	366	364	
$T(A_1)$	203	198	144	150	161	202	188	188 ± 2
				$(DF)_\infty$				
$S(B_1)$	2400	2553	3063	3023	2666	2530	2511	2506 ± 4
$S(A_1)$	2089	2272	2940	2874	2432	2294	2281	2272 ± 6
$L(B_1)$	803	790	627	728	741	720	703	
$L(B_2)$	574	576	482	519	628	572	552	564 ± 4
$L(A_2)$	511	512	415	399	516	inactive	492	515 ± 3
$L(A_1)$	478	476	383	429	498	403	417	409 ± 3
$T(B_1)$	402	400	305	378	479	355	359	
$T(A_1)$	201	196	142	149	160	210	190	192 ± 2

[a] Obtained in this study using the 6-311++G(d,p) basis set. [b] Obtained by Beyer and Karpfen (ref 37) with basis set II (see text). [c] Obtained by Beyer and Karpfen (ref 37) with basis set I (see text). [d] Reference 25. [e] Reference 26. [f] Reference 30.

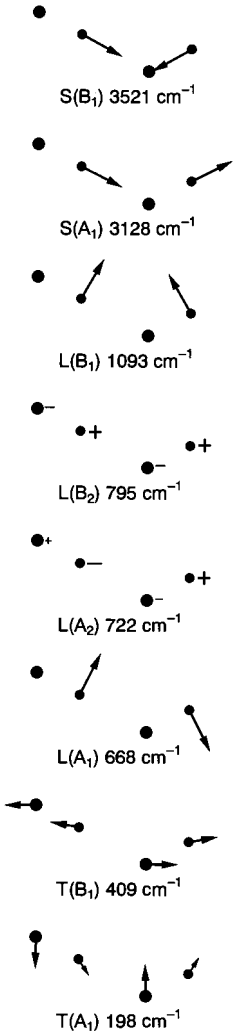

Figure 4. Normal coordinates of the infrared- and Raman-active modes of hydrogen fluoride polymer. Larger filled circles represent fluorine nuclei and smaller ones hydrogen nuclei. The numbers indicate the frequencies calculated at the B3LYP level.

polymer. From the experimental side, the frequency shift is 894 (=3961−3067) cm^{-1} for the $S(A_1)$ mode of $(HF)_\infty$. The shift calculated at the RHF level is 437 cm^{-1}, which amounts to only 49% of the experimental value. The BLYP level, on the contrary, yields the calculated splittings [436 and 311 cm^{-1} for $(HF)_\infty$ and $(DF)_\infty$, respectively], which are larger than the experimental values (340 and 230 cm^{-1}). Therefore, the BLYP level overestimates the hydrogen-bond interactions. Furthermore, the downward shift in the frequencies of the H−F stretching mode from the monomer to the polymer is also overestimated; the BLYP calculations predict too large a shift of 1065 cm^{-1} as compared with the experimental value (894 cm^{-1}), although the deviation becomes much smaller at the BLYP level than at the RHF level. The use of the B3LYP functional leads to significantly improved agreements in this frequency region. The calculated frequencies of the $S(A_1)$ and $S(B_1)$ modes seem reasonable as compared with the experiments. The calculated splittings of these two modes [393 and 281 cm^{-1} for $(HF)_\infty$ and $(DF)_\infty$, respectively] become much closer to the experimental values (340 and 230 cm^{-1}), and the calculated downward shift (970 cm^{-1}) is also in better agreement with the observed value (894 cm^{-1}) than that obtained at the RHF or BLYP level. Therefore, the chain-length dependence predicted at the B3LYP level is reasonable although it is still slightly overestimated.

There are two pseudo-translational vibrations in the region below 400 cm^{-1}. In the $T(A_1)$ mode, the HF units move nearly perpendicular to the chain axis, while in the $T(B_1)$ mode, the displacements are along the chain axis (see Figure 4). The frequencies of these modes calculated at the RHF level are lower than the experimental values, while those obtained at the BLYP and B3LYP levels, which agree with each other, are higher than the observed. As expected from their vibrational patterns, the frequencies of the pseudo-translational modes are relatively insensitive to the deuteration. The observed frequency of the $T(B_1)$ mode of $(DF)_\infty$ is slightly lower than that of $(HF)_\infty$. The calculated frequencies are consistent with this observed small downward shift upon deuteration. In contrast to $T(B_1)$ mode, the frequency of $T(A_1)$ mode becomes higher upon deuteration. This upward shift cannot be explained by the single chain approximation employed in this study; the interchain interactions probably play a role in this upward shift.

The $T(A_1)$ mode can be regarded as the in-phase stretching motion of the H···F hydrogen bonds. This motion is expected to couple strongly with the intramolecular H−F stretching (S)

modes, because the changes in the H···F hydrogen-bond distances substantially affect the shape of the potential energy curves along the H−F stretching coordinates. The weak bands observed in the 2000−4000 cm^{-1} region of HF and DF crystals are combination tones of $S(A_1)$ and $T(A_1)$ and of $S(B_1)$ and $T(A_1)$.[25] Marechal and Witkowski[81] have analyzed the broad and complex infrared spectral band profiles of general hydrogen-bonded systems in terms of the coupling between the intramolecular high-frequency X−H stretching modes and the low-frequency X−H···Y hydrogen-bond stretching modes. The theoretical model developed by Marechal and Witkowski is capable of predicting the spectral band profiles and their changes upon isotopic substitution, and Wójcik has successfully applied the model to various hydrogen-bonded complexes and crystals.[82,83] We point out that this model can also be invoked to explain the observed behavior of the combination bands in HF and DF crystals. For instance, the phenomena that the combination bands in DF crystals are much less intense than in HF crystals and that the combination bands associated with $T(B_1)$ modes are not observed are readily accounted for by this model.

Four fundamental normal modes are expected in the librational (400−2000 cm^{-1}) region. However, there have been found more than four peaks in the observed infrared and Raman spectra in this region, and some of these peaks are very broad, which complicates the assignments. The frequencies of the librational modes calculated at the BLYP and B3LYP levels are in good agreement with each other, while those calculated at the RHF level are significantly lower than the density functional results. The assignment made on the basis of these calculated frequencies is given in Table 9. The observed frequency of each librational mode falls within the frequency region bracketed by the density functional and RHF results. The RHF level invariably underestimates the frequencies of the librational modes. The frequencies calculated at the BLYP and B3LYP levels are in reasonable agreement with the observed frequencies, although some of them are significantly overestimated. These results are consistent with our previous conclusion that the RHF level underestimates the chain-length dependence of the frequencies, whereas the BLYP and B3LYP levels slightly overestimate it.

Our assignment generally agrees with the previous one made by Anderson et al.[26,27] except for a few modes. In the paper published in 1980, Anderson et al.[26] assigned a Raman band at 742 cm^{-1} to $L(B_1)$ and a band at 943 cm^{-1} to $L(B_2)$ for $(HF)_\infty$ and likewise for $(DF)_\infty$. Pinnick et al.[30] supported this assignment. Our calculations indicate that the frequencies of $L(B_1)$ modes are higher than those of the $L(B_2)$ modes, and accordingly in the table we have reversed the assignment of these modes made by Anderson et al. In the paper of 1981, Anderson et al.[27] changed their assignment in the librational frequency region, such that the assignment of $L(B_1)$ and $L(B_2)$ modes is the same as ours. However, they also reversed the assignment of $L(A_1)$ and $L(A_2)$ modes on the basis of their normal coordinate analysis. Our calculations suggest, however, that their previous assignment for $L(A_1)$ and $L(A_2)$ modes is more reasonable. The intensities of the infrared bands at 792 cm^{-1} of HF crystals and at 572 cm^{-1} of DF crystals are strongly dependent on the conditions of crystallization. Kittelberger and Hornig[25] suggested that these bands manifested itself due to the formation of imperfect crystals and are disorder-induced modes. Pinnick et al.,[30] however, argued that these modes are true fundamental librational modes on the basis of the morphology of the crystal growth. The frequencies of $L(B_2)$ modes calculated at the B3LYP level are 795 cm^{-1} for $(HF)_\infty$ and 576 cm^{-1} for $(DF)_\infty$, respectively, and are in good agreement with the observed frequencies of these modes. This result seems to support the view of Pinnick et al.

Conclusion

Optimized structures and vibrational frequencies are obtained for linear HF oligomers and an infinite zigzag HF polymer using ab initio molecular orbital and crystal orbital theories. It is demonstrated that electron correlation, as taken into account at the BLYP and B3LYP levels, has profound effects not only on the absolute values of the structural parameters, binding energies, and vibrational frequencies but also on their chain-length dependence, which results from the cooperativity of the consecutive hydrogen bonds. The RHF level significantly underestimates the cooperativity. Too short an H−F bond length, too long F···H and H···H distances, and too high frequencies of the H−F and D−F stretching modes of $(HF)_\infty$ and $(DF)_\infty$ predicted at the RHF level are at least partly ascribable to this deficiency. The chain-length dependence of the structural parameters and vibrational frequencies predicted at the BLYP and B3LYP levels is reasonable as compared with the experimental data or the results obtained from the MP2 calculations. The BLYP level yields too low frequencies for the H−F stretching mode of the isolated monomer, and this tendency is carried over to the results for $(HF)_\infty$ and $(DF)_\infty$. The B3LYP functional reproduces the H−F stretching frequencies of the monomer and polymer reasonably well. The downward frequency shifts in the stretching modes are overestimated at the BLYP and B3LYP levels, but the agreements are significantly better at the BLYP and B3LYP levels than at the RHF level. The BLYP and B3LYP levels reproduce the structural parameters of $(HF)_\infty$ with considerable accuracy. On this basis, we conclude that the BLYP and B3LYP levels describe reasonably well but slightly overestimate the cooperativity of the consecutive hydrogen bonds, whereas the RHF level greatly underestimates this property. The overestimation at the BLYP and B3LYP levels is at least partly ascribable to BSSE.

The results obtained from MP2 calculations for the binding energies, structural parameters, and vibrational frequencies very often fall between the RHF and density functional results. The MP2 results are generally in good agreement with the experimental data for HF monomer and dimer. Thus, we are inclined to expect that the crystal orbital calculations at the MP2 level would provide us with good structural parameters and vibrational frequencies for $(HF)_\infty$. However, considering that a relatively large part (about 20%) of the binding energies at the MP2 level is BSSE, we expect that the "BSSE-corrected" MP2 results for $(HF)_\infty$ will probably be better than the "BSSE-corrected" RHF results, but they will not be as good as "BSSE-corrected" density functional results. This expectation does not necessarily contradict with the previous conclusion that electron correlation plays an essential role in cooperative binding effects.

Vibrational assignment of the infrared and Raman bands in the librational frequency region is reexamined on the basis of the present calculations. We reversed the assignment of $L(B_1)$ and $L(B_2)$ modes made by Anderson et al.[26] The frequencies of the librational and pseudo-translational modes calculated at the RHF levels are lower than the observed. The BLYP and B3LYP levels reproduce the experimental results reasonably well, but they tend to overestimate the frequencies of some modes. Consequently, the observed frequency of each mode falls between the corresponding frequencies calculated at the

RHF and density functional levels. These results are consistent with the underestimation of the chain-length dependence of the vibrational frequencies at the RHF levels and the slight overestimation at the BLYP and B3LYP levels.

Acknowledgment. The authors gratefully acknowledge Dr. Mikhail V. Vener for critical reading of the manuscript and helpful discussions. The authors would like to thank Professor Alfred Karpfen for providing us with his recent publication dealing with HF clusters. One of the authors (S.H.) is indebted to the Japan Society for the Promotion of Science for a Research Fellowship for Young Scientists. The present work was partly supported by the Grant-in-Aids for Scientific Research (A) (No. 09304057) by the Ministry of Education, Science, Sports, and Culture, Japan.

Appendix

In the framework of spin-restricted hybrid Hartree−Fock/density functional crystal orbital theory of polymers,[63,84] Kohn−Sham crystal (Bloch) orbitals are expressed as linear combinations of atomic orbitals $\chi_\mu^{(q)}(\boldsymbol{r})$ in the form

$$\psi_n^{[k]}(\mathbf{r}) = \frac{1}{\sqrt{K}} \sum_\mu \sum_q C_{\mu n}^{[k]} \exp(ikqa) \chi_\mu^{(q)}(\mathbf{r}) \tag{1}$$

where a is the translational period, and K is the number of unit cells in the system. The crystal orbital $\psi_n^{[k]}(\boldsymbol{r})$ and crystal orbital coefficient $C_{\mu n}^{[k]}$ are characterized by energy band n and quasi-momentum k, which are indicated by subscripts and square-bracketed superscripts, respectively. The atomic orbital $\chi_\mu^{(q)}(\boldsymbol{r})$ is a real spatial function centered in unit cell q.

By using the above-mentioned symmetry-adapted basis functions and applying Ritz variation principle to the total energy expectation value, we obtain the following k-dependent Hartree−Fock−Roothaan equation[31−34]

$$\mathbf{F}^{[k]}\mathbf{C}^{[k]} = \mathbf{S}^{[k]}\mathbf{C}^{[k]}\epsilon^{[k]} \tag{2}$$

where $\epsilon^{[k]}$ is a diagonal matrix of one-electron energies. The elements of the k-dependent Fock and overlap matrixes are defined as

$$F_{\mu\nu}^{[k]} = \sum_q F_{\mu\nu}^{(q)} \exp(ikqa) \tag{3}$$

and

$$S_{\mu\nu}^{[k]} = \sum_q S_{\mu\nu}^{(q)} \exp(ikqa) \tag{4}$$

where

$$F_{\mu\nu}^{(q)} = H_{\mu\nu}^{(q)} + \sum_{\lambda,\sigma}\sum_{r,s} P_{\lambda\sigma}^{(s-r)} (\mu^{(0)}\nu^{(q)}|\lambda^{(r)}\sigma^{(s)}) + m_1 X_{\mu\nu}^{(q)} - \frac{m_2}{2} \sum_{\lambda,\sigma}\sum_{r,s} P_{\lambda\sigma}^{(s-r)} (\mu^{(0)}\lambda^{(r)}|\nu^{(q)}\sigma^{(s)}) + M_{\mu\nu}^{(q)} \tag{5}$$

and

$$S_{\mu\nu}^{(q)} = \int \chi_\mu^{(0)}(\mathbf{r}) \chi_\nu^{(q)}(\mathbf{r}) d\mathbf{r} \tag{6}$$

Lattice summations in eq 5 are truncated after several terms, and the long-range electrostatic contributions $M_{\mu\nu}^{(q)}$ to the Fock matrix elements are estimated by the multipole expansion technique.[66] The matrix H in eq 5 is the one-electron part of the Fock matrix, whose elements are given by

$$H_{\mu\nu}^{(q)} = \int \chi_\mu^{(0)}(\mathbf{r}) \left(-\frac{1}{2}\nabla^2\right) \chi_\nu^{(q)}(\mathbf{r}) d\mathbf{r} - \sum_A \sum_r \int \chi_\mu^{(0)}(\mathbf{r}) \frac{Z_A}{|\mathbf{r} - \mathbf{R}_A^{(r)}|} \chi_\nu^{(q)}(\mathbf{r}) d\mathbf{r} \tag{7}$$

where Z_A is the charge of nucleus A at position $\mathbf{R}_A^{(r)}$. The elements of the density matrix $P_{\mu\nu}^{(q)}$ are defined as

$$P_{\mu\nu}^{(q)} = \frac{2}{K} \sum_j^{\text{occ. BZ}} \sum_k C_{\mu j}^{[k]*} C_{\nu j}^{[k]} \exp(ikqa) \tag{8}$$

where the summations are over all the occupied states in the first Brillouin zone. Two-electron integrals $(\mu^{(0)}\nu^{(q)}|\lambda^{(r)}\sigma^{(s)})$ in eq 5 are

$$(\mu^{(0)}\nu^{(q)}|\lambda^{(r)}\sigma^{(s)}) = \int\int \chi_\mu^{(0)}(\mathbf{r}_1) \chi_\nu^{(q)}(\mathbf{r}_1) \frac{1}{r_{12}} \chi_\lambda^{(r)}(\mathbf{r}_2) \chi_\sigma^{(s)}(\mathbf{r}_2) d\mathbf{r}_1 d\mathbf{r}_2 \tag{9}$$

Parameters m_1 and m_2 in eq 5 denote the mixing ratios of exchange-correlation energy and exact-exchange energy, respectively. In practice, more than one exchange-correlation functional is used in hybrid exchange-correlation functionals such as in the B3LYP functional.[49] We assume that the exchange-correlation functional has the form

$$f = f(\rho, \nabla\rho) \tag{10}$$

where ρ and $\nabla\rho$ are electron density and its gradient. The elements of the exchange-correlation part $X_{\mu\nu}^{(q)}$ of the Fock matrix are given by[85,86]

$$X_{\mu\nu}^{(q)} = \int \{\chi_\mu^{(0)} v_{\text{xc}} \chi_\nu^{(q)} + \nabla\chi_\mu^{(0)} \cdot \mathbf{g}_{\text{xc}} \chi_\nu^{(q)} + \chi_\mu^{(0)} \mathbf{g}_{\text{xc}} \cdot \nabla\chi_\nu^{(q)}\} d\mathbf{r} \tag{11}$$

with

$$v_{\text{xc}} = \frac{\partial f}{\partial \rho} \tag{12}$$

$$\mathbf{g}_{\text{xc}} = \left\{\frac{\partial f}{\partial \gamma_{\alpha\alpha}} + \frac{1}{2}\frac{\partial f}{\partial \gamma_{\alpha\beta}}\right\} \nabla\rho \tag{13}$$

$$\gamma_{\alpha\alpha} = \nabla\rho_\alpha \cdot \nabla\rho_\alpha \tag{14}$$

$$\gamma_{\alpha\beta} = \nabla\rho_\alpha \cdot \nabla\rho_\beta \tag{15}$$

where α and β denote spins.

The total energy per unit cell is then expressed as

$$E = \sum_{\mu,\nu}\sum_q P_{\mu\nu}^{(q)} H_{\mu\nu}^{(q)} + \frac{1}{2} \sum_{\mu,\nu}\sum_{\lambda,\sigma}\sum_{q,r,s} P_{\mu\nu}^{(q)} P_{\lambda\sigma}^{(s-r)} \times (\mu^{(0)}\nu^{(q)}|\lambda^{(r)}\sigma^{(s)}) + m_1 \int_{\text{cell}} f(\rho, \nabla\rho)\, d\mathbf{r} - \frac{m_2}{4} \sum_{\mu,\nu}\sum_{\lambda,\sigma}\sum_{q,r,s} P_{\mu\nu}^{(q)} P_{\lambda\sigma}^{(s-r)} (\mu^{(0)}\lambda^{(r)}|\nu^{(q)}\sigma^{(s)}) + E_{\text{ME}} + E_{\text{NR}} \tag{16}$$

where E_{ME} and E_{NR} are multipole expansion correction and nuclear repulsion energy per unit cell, respectively. The energy gradients with respect to an in-phase ($k = 0$) nuclear coordinate Q can be obtained by directly differentiating eq 16. The evaluation of the derivatives of orbital coefficients can be

avoided by using the orthonormality condition of crystal orbitals[59−61]

$$\frac{\partial E}{\partial Q} = \sum_{\mu,\nu}\sum_{q} P_{\mu\nu}^{(q)} \frac{\partial H_{\mu\nu}^{(q)}}{\partial Q} + \frac{1}{2}\sum_{\mu,\nu}\sum_{\lambda,\sigma}\sum_{q,r,s} P_{\mu\nu}^{(q)} P_{\lambda\sigma}^{(s-r)} \frac{\partial}{\partial Q} \times (\mu^{(0)}\nu^{(q)}|\lambda^{(r)}\sigma^{(s)}) + m_1 \sum_{\mu,\nu}\sum_{q} P_{\mu\nu}^{(q)} \int \left\{ \chi_\mu^{(0)} v_{xc} \frac{\partial \chi_\nu^{(q)}}{\partial Q} + \frac{\partial \chi_\mu^{(0)}}{\partial Q} v_{xc} \chi_\nu^{(q)} + \nabla\chi_\mu^{(0)} \cdot \mathbf{g}_{xc} \frac{\partial \chi_\nu^{(q)}}{\partial Q} + \frac{\partial \nabla\chi_\mu^{(0)}}{\partial Q} \cdot \mathbf{g}_{xc} \chi_\nu^{(q)} + \chi_\mu^{(0)} \mathbf{g}_{xc} \cdot \frac{\partial \nabla\chi_\nu^{(q)}}{\partial Q} + \frac{\partial \chi_\mu^{(0)}}{\partial Q} \mathbf{g}_{xc} \cdot \nabla\chi_\nu^{(q)} \right\} d\mathbf{r} - \frac{m_2}{4} \sum_{\mu,\nu}\sum_{\lambda,\sigma}\sum_{q,r,s} P_{\mu\nu}^{(q)} P_{\lambda\sigma}^{(s-r)} \frac{\partial}{\partial Q} (\mu^{(0)}\lambda^{(r)}|\nu^{(q)}\sigma^{(s)}) + \frac{\partial E_{NR}}{\partial Q} - \sum_{\mu,\nu}\sum_{q} W_{\mu\nu}^{(q)} \frac{\partial S_{\mu\nu}^{(q)}}{\partial Q} \quad (17)$$

where W is the energy-weighted density matrix, whose elements are defined as

$$W_{\mu\nu}^{(q)} = \frac{2}{K} \sum_{j}^{\text{occ. BZ}} \sum_{k} \epsilon_j^{[k]} C_{\mu j}^{[k]*} C_{\nu j}^{[k]} \exp(ikqa) \quad (18)$$

Since the first (and higher) derivatives of total energy are expected to converge much faster than the total energy itself, we neglect the gradient contributions from the multipole expansion correction. For instance, the leading term in the expression for the dipole−dipole interaction energy is proportional to $1/r^3$ with r being the distance between the centers of two dipoles. The forces resulting from the dipole−dipole interaction are then proportional to $1/r$,[4] and hence they converge more rapidly than the interaction energy itself with increasing r.

The analytical energy gradient with respect to the translational period a can be calculated by using eq 17 and the following relation:[59−61]

$$\frac{\partial}{\partial a} = \sum_{A}\sum_{q} q \frac{\partial}{\partial Q_z^{A(q)}} \quad (19)$$

Here $Q_z^{A(q)}$ denotes the z-coordinate, which we assume to be parallel to the chain axis, of nucleus A in unit cell q. The differentiation of exchange-correlation part of the energy with respect to a gives rise to a two-dimensional (surface) integral.[61] This two-dimensional integral can be transformed to three-dimensional (volume) integrals by virtue of Gauss theorem,[61] and these three-dimensional integrals are conveniently evaluated by using the atomic partitioning scheme of Becke.[87]

References and Notes

(1) Frank, H. S. *Proc. R. Soc. (London) A* **1958,** *247,* 481.
(2) Del Bene, J.; Pople, J. A. *J. Chem. Phys.* **1970,** *52,* 4858.
(3) Del Bene, J. E.; Pople, J. A. *J. Chem. Phys.* **1971,** *55,* 2296.
(4) Del Bene, J. E.; Pople, J. A. *J. Chem. Phys.* **1973,** *58,* 3605.
(5) Schuster, P.; Zundel, G.; Sandorfy, C. *The Hydrogen Bond;* North-Holland: Amsterdam, 1976; Vols. 1−3.
(6) Jeffrey, G. A.; Gress, M. E.; Takagi, S. *J. Am. Chem. Soc.* **1977,** *99,* 609.
(7) Tse, Y.-C.; Newton, M. D. *J. Am. Chem. Soc.* **1977,** *99,* 611.
(8) Jeffrey, G. A.; Saenger, W. *Hydrogen Bonding in Biological Structures;* Springer-Verlag: Berlin, 1991.
(9) Latajka, Z.; Scheiner, S. *Chem. Phys.* **1988,** *122,* 413.
(10) Nesbitt, D. J. *Chem. Rev.* **1988,** *88,* 843.
(11) Chałasiński, G.; Cybulski, S. M.; Szczęśniak, M. M.; Scheiner, S. *J. Chem. Phys.* **1989,** *91,* 7048.
(12) Karpfen, A. *Int. J. Quantum Chem. Quantum Chem. Symp.* **1990,** *24,* 129.
(13) Quack, M.; Stohner, J.; Suhm, M. A. *J. Mol. Struct.* **1993,** *294,* 33.
(14) Karpfen, A.; Yanovitskii, O. *J. Mol. Struct. (THEOCHEM)* **1994,** *307,* 81.
(15) Karpfen, A.; Yanovitskii, O. *J. Mol. Struct. (THEOCHEM)* **1994,** *314,* 211.
(16) Liedl, K. R.; Kroemer, R. T.; Rode, B. M. *Chem. Phys. Lett.* **1995,** *246,* 455.
(17) Karpfen, A. In *Molecular Interactions;* Scheiner, S., Ed., Wiley: 1997; p 265.
(18) Atoji, M.; Lipscomb, W. N. *Acta Crystallogr.* **1954,** *7,* 173.
(19) Johnson, M. W.; Sándor, E.; Arzi, E. *Acta Crystallogr. B* **1975,** *31,* 1998.
(20) Sastri, M. L. N.; Hornig, D. F. *J. Chem. Phys.* **1963,** *39,* 3497.
(21) Dyke, T. R.; Howard, B. J.; Klemperer, W. *J. Chem. Phys.* **1972,** *56,* 2442.
(22) Howard, B. J.; Dyke, T. R.; Klemperer, W. *J. Chem. Phys.* **1984,** *81,* 5417.
(23) Pine, A. S.; Lafferty, W. J. *J. Chem. Phys.* **1983,** *78,* 2154.
(24) Giguère, P. A.; Zengin, N. *Can. J. Chem.* **1958,** *36,* 1013.
(25) Kittelberger, J. S.; Hornig, D. F. *J. Chem. Phys.* **1967,** *46,* 3099.
(26) Anderson, A.; Torrie, B. H.; Tse, W. S. *Chem. Phys. Lett.* **1980,** *70,* 300.
(27) Anderson, A.; Torrie, B. H.; Tse, W. S. *J. Raman Spectrosc.* **1981,** *10,* 148.
(28) Lee, S. A.; Pinnick, D. A.; Lindsay, S. M.; Hanson, R. C. *Phys. Rev. B* **1986,** *34,* 2799.
(29) Jansen, R. W.; Bertoncini, R.; Pinnick, D. A.; Katz, A. I.; Hanson, R. C.; Sankey, O. F.; O'Keeffe, M. *Phys. Rev. B* **1987,** *35,* 9830.
(30) Pinnick, D. A.; Katz, A. I.; Hanson, R. C. *Phys. Rev. B* **1989,** *39,* 8677.
(31) Del Re, G.; Ladik, J.; Biczó, G. *Phys. Rev.* **1967,** *155,* 997.
(32) André, J. M. *J. Chem. Phys.* **1969,** *50,* 1536.
(33) Kertész, M. *Adv. Quantum Chem.* **1982,** *15,* 161.
(34) Ladik, J. J. *Quantum Theory of Polymers as Solids;* Plenum: New York, 1988.
(35) Kertész, M.; Koller, J.; Azman, A. *Chem. Phys. Lett.* **1975,** *36,* 576.
(36) Karpfen, A.; Beyer, A.; Schuster, P. *Int. J. Quantum Chem.* **1981,** *19,* 1113.
(37) Beyer, A.; Karpfen, A. *Chem. Phys.* **1982,** *64,* 343.
(38) I'haya, Y. J.; Narita, S.; Fujita, Y.; Ujino, H. *Int. J. Quantum Chem. Quantum Chem. Symp.* **1984,** *18,* 153.
(39) Liegener, C.-M.; Ladik, J. *Phys. Rev. B* **1987,** *35,* 6403.
(40) Berski, S.; Latajka, Z. *J. Mol. Struct. (THEOCHEM)* **1997,** *389,* 147.
(41) Mayer, I.; Räther, G.; Suhai, S. *Chem. Phys. Lett.* **1997,** *270,* 211.
(42) Springborg, M. *Phys. Rev. Lett.* **1987,** *59,* 2287.
(43) Springborg, M. *Phys. Rev. B* **1988,** *38,* 1483.
(44) Scheiner, S. In *Theoretical Models of Chemical Bonding;* Maksić, Z. B., Ed., Springer-Verlag: Berlin, 1991; Part 4, p 171.
(45) Truhlar, D. G. In *Dynamics of Polyatomic van der Waals Complexes;* Halberstadt, N., Janda, K. C., Eds., Plenum: New York, 1990; p 159.
(46) Becke, A. D. *Phys. Rev. A* **1988,** *38,* 3098.
(47) Lee, C.; Yang, W.; Parr, R. G. *Phys. Rev. B* **1988,** *37,* 785.
(48) Miehlich, B.; Savin, A.; Stoll, H.; Preuss, H. *Chem. Phys. Lett.* **1989,** *157,* 200.
(49) Becke, A. D. *J. Chem. Phys.* **1993,** *98,* 5648.
(50) To avoid confusion, we use different abbreviations for hydrogen fluoride (HF) and for Hartree−Fock (RHF).
(51) Latajka, Z.; Bouteiller, Y. *J. Chem. Phys.* **1994,** *101,* 9793.
(52) Jeanvoine, Y.; Bohr, F.; Ruiz-López, M. F. *Can. J. Chem.* **1995,** *73,* 710.
(53) Hobza, P.; Šponer, J.; Reschel, T. *J. Comput. Chem.* **1995,** *16,* 1315.
(54) Gaussian 94, Revision E.2.; Frisch, M. J.; Trucks, G. W.; Schlegel, H. B.; Gill, P. M. W.; Johnson, B. G.; Robb, M. A.; Cheeseman, J. R.; Keith, T.; Petersson, G. A.; Montgomery, J. A.; Raghavachari, K.; Al-Laham, M. A.; Zakrzewski, V. G.; Ortiz, J. V.; Foresman, J. B.; Cioslowski, J.; Stefanov, B. B.; Nanayakkara, A.; Challacombe, M.; Peng, C. Y.; Ayala, P. Y.; Chen, W.; Wong, M. W.; Andres, J. L.; Replogle, E. S.; Gomperts, R.; Martin, R. L.; Fox, D. J.; Binkley, J. S.; Defrees, D. J.; Baker, J.; Stewart, J. P.; Head-Gordon, M.; Gonzalez, C.; Pople, J. A. Gaussian, Inc.: Pittsburgh, PA, 1995.
(55) Shore, B. W. *J. Chem. Phys.* **1973,** *59,* 6450.
(56) Boys, S. F.; Bernardi, F. *Mol. Phys.* **1970,** *19,* 553.
(57) Mayer, I.; Surján, P. R. *Chem. Phys. Lett.* **1992,** *191,* 497.
(58) Turi, L.; Dannenberg, J. J. *J. Phys. Chem.* **1993,** *97,* 2488.

(59) Teramae, H.; Yamabe, T.; Satoko, C.; Imamura, A. *Chem. Phys. Lett.* **1983,** *101,* 149.
(60) Teramae, H.; Yamabe, T.; Imamura, A. *J. Chem. Phys.* **1984,** *81,* 3564.
(61) Hirata, S.; Iwata, S. *J. Chem. Phys.* **1997,** *107,* 10075.
(62) Hirata, S.; Iwata, S. *J. Chem. Phys.* **1998,** *108,* 7901.
(63) Hirata, S.; Torii, H.; Tasumi, M. *Phys. Rev. B* **1998,** *57,* 11994.
(64) Dunlap, B. I.; Connolly, J. W. D.; Sabin, J. R. *J. Chem. Phys.* **1979,** *71,* 3396.
(65) Dunlap, B. I.; Connolly, J. W. D.; Sabin, J. R. *J. Chem. Phys.* **1979,** *71,* 4993.
(66) Delhalle, J.; Piela, L.; Brédas, J.-L.; André, J.-M. *Phys. Rev. B* **1980,** *22,* 6254.
(67) André, J. M.; Vercauteren, D. P.; Bodart, V. P.; Fripiat, J. G. *J. Comput. Chem.* **1984,** *5,* 535.
(68) Huber, K. P.; Herzberg, G. *Molecular Spectra and Molecular Structure IV. Constants of Diatomic Molecules;* Van Nostrand Reinhold: New York, 1979.
(69) Gutowsky, H. S.; Chuang, C.; Keen, J. D.; Klots, T. D.; Emilsson, T. *J. Chem. Phys.* **1985,** *83,* 2070.
(70) Habuda, S. P.; Gagarinsky, Yu. V. *Acta Crystallogr. B* **1971,** *27,* 1677.
(71) Pine, A. S.; Howard, B. J. *J. Chem. Phys.* **1986,** *84,* 590.
(72) Dayton, D. C.; Jucks, K. W.; Miller, R. E. *J. Chem. Phys.* **1989,** *90,* 2631.
(73) Guelachvili, G. *Opt. Commun.* **1976,** *19,* 150.
(74) von Puttkamer, K.; Quack, M. *Chem. Phys.* **1989,** *139,* 31.
(75) Andrews, L.; Johnson, G. L. *J. Phys. Chem.* **1984,** *88,* 425.
(76) Hunt, R. D.; Andrews, L. *J. Chem. Phys.* **1985,** *82,* 4442.
(77) Andrews, L.; Davis, S. R.; Hunt, R. D. *Mol. Phys.* **1992,** *77,* 993.
(78) Boutin, H.; Safford, G. J.; Brajovic, V. *J. Chem. Phys.* **1963,** *39,* 3135.
(79) Axmann, A.; Biem, W.; Borsch, P.; Hossfeld, F.; Stiller, H. *Discuss. Faraday Soc.* **1969,** *48,* 69.
(80) Tubino, R.; Zerbi, G. *J. Chem. Phys.* **1969,** *51,* 4509.
(81) Marechal, Y.; Witkowski, A. *J. Chem. Phys.* **1968,** *48,* 3697.
(82) Wójcik, M. J. *Int. J. Quantum. Chem.* **1976,** *10,* 747.
(83) Wójcik, M. J. *Int. J. Quantum. Chem.* **1986,** *29,* 855.
(84) Suhai, S. *Phys. Rev. B* **1995,** *51,* 16553.
(85) Pople, J. A.; Gill, P. M. W.; Johnson, B. G. *Chem. Phys. Lett.* **1992,** *199,* 557.
(86) Johnson, B. G.; Gill, P. M. W.; Pople, J. A. *J. Chem. Phys.* **1993,** *98,* 5612.
(87) Becke, A. D. *J. Chem. Phys.* **1988,** *88,* 2547.